

# CMS Search Plans and Sensitivity to New Physics with Dijets

The CMS Collaboration

## Abstract

1 CMS will use dijets to search for physics beyond the standard model during early LHC  
2 running. The inclusive jet cross section as a function of jet transverse momentum with  
3  $10 \text{ pb}^{-1}$  of integrated luminosity is sensitive to contact interactions beyond the reach of  
4 the Tevatron. The dijet mass distribution will be used to search for dijet resonances such  
5 as an excited quark. Additional sensitivity to the existence of contact interactions or  
6 dijet resonances can be obtained by comparing dijet rates in two distinct pseudorapidity  
7 regions.

8 The Large Hadron Collider at CERN will produce many events with two energetic  
9 jets resulting from proton-proton collisions at  $\sqrt{s} = 14$  TeV. These dijet events result  
10 from parton scattering, produced by the strong interaction of quarks ( $q$ ) and gluons ( $g$ )  
11 inside the protons. This paper discusses plans to use dijets in the search for two signals  
12 of new physics: contact interactions and resonances decaying into dijets. This generic  
13 search is applied to two models of quark compositeness, that are used as benchmarks  
14 of sensitivity to new physics. The first model is a contact interaction [1] among left-  
15 handed quarks at an energy scale  $\Lambda^+$  in the process  $qq \rightarrow qq$ , modeled with the effective  
16 Lagrangian  $L_{qq} = (\pm 2\pi\alpha_s/\Lambda^2)(\bar{q}_L\gamma^\mu q_L)(\bar{q}_L\gamma_\mu q_L)$  with  $+$  chosen for the sign. The second  
17 model is a dijet resonance signal from the decay of an excited quark ( $q^*$ ) [2] in the process  
18  $qq \rightarrow q^* \rightarrow qq$ . All processes presented here have been simulated using PYTHIA version  
19 6.4 [3].

20 A detailed description of the Compact Muon Solenoid (CMS) experiment can be found  
21 elsewhere [4, 5]. The CMS coordinate system has the origin at the center of the detector,  
22  $z$ -axis points along the beam direction toward the Jura mountains, transverse direction  
23 perpendicular to the beam, azimuthal angle  $\phi$ , polar angle  $\theta$ , and pseudorapidity  $\eta =$   
24  $-\ln(\tan[\theta/2])$ . The central feature of the CMS apparatus is a superconducting solenoid,  
25 of 6m internal diameter. Within the field volume are the silicon pixel and strip tracker, and  
26 the barrel and endcap calorimeters. The crystal electromagnetic calorimeter (ECAL) and  
27 the brass-scintillator hadronic calorimeter (HCAL) are in the barrel and endcap ( $|\eta| < 3$ ).  
28 Outside the field volume in the forward region is an iron-quartz fiber hadronic calorimeter

29 ( $3 < |\eta| < 5$ ). The HCAL and ECAL cells are grouped into towers, projecting radially  
 30 outward from the origin, for triggering purposes and to facilitate the jet reconstruction. In  
 31 the region  $|\eta| < 1.74$  these projective calorimeter towers have segmentation  $\Delta\eta = \Delta\phi =$   
 32  $0.087$ , and the  $\eta$  and  $\phi$  width progressively increases at higher values of  $\eta$ . The energy  
 33 in the HCAL and ECAL within each projective tower is summed to find the calorimeter  
 34 tower energy. Towers with  $|\eta| < 1.3$  contain only cells from the barrel calorimeters, towers  
 35 in the transition region  $1.3 < |\eta| < 1.5$  contain a mixture of barrel and endcap cells, and  
 36 towers in the region  $1.5 < |\eta| < 3.0$  contain only cells from the endcap calorimeters.

37 Jets are reconstructed using both the iterative and midpoint cone algorithms [5], with  
 38 indistinguishable results for this analysis. Below we will discuss three types of jets: recon-  
 39 structed, corrected and generated. The reconstructed jet energy,  $E$ , is defined as the scalar  
 40 sum of the calorimeter tower energies inside a cone of radius  $\sqrt{(\Delta\eta)^2 + (\Delta\phi)^2} = 0.5$ , cen-  
 41 tered on the jet axis. The jet momentum,  $\vec{p}$ , is the corresponding vector sum:  $\vec{p} = \sum E_i \hat{u}_i$   
 42 with  $\hat{u}_i$  being the unit vector pointing from the origin to the energy deposition  $E_i$  inside  
 43 the same cone. Jet transverse momentum,  $p_T$ , is the component of  $\vec{p}$  in the transverse  
 44 direction. The  $E$  and  $\vec{p}$  of a reconstructed jet are then corrected for the non-linear re-  
 45 sponse of the calorimeter to a generated jet. Generated jets come from applying the  
 46 same jet algorithm to the Lorentz vectors of stable generated particles before detector  
 47 simulation. The  $p_T$  of a corrected jet is equal to the  $p_T$  of the corresponding generated  
 48 jet on average. The jet corrections estimated from a GEANT [6] simulation of the CMS  
 49 detector increase the jet  $p_T$  on average by roughly 50% (10%) for 70 GeV (3 TeV) jets

50 in the region  $|\eta| < 1.3$ . Further details on jet reconstruction and jet energy corrections  
51 can be found elsewhere [5, 7]. The jet measurements presented here are within the region  
52  $|\eta| < 1.3$ , where there is expected to be the highest sensitivity to new physics, and where  
53 the reconstructed jet response variations as a function of  $\eta$  are both moderate and smooth.

54 The dijet system is defined to be the two jets with the highest  $p_T$  in an event (leading  
55 jets), and the dijet mass is given by  $m = \sqrt{(E_1 + E_2)^2 - (\vec{p}_1 + \vec{p}_2)^2}$ . The estimated dijet  
56 mass resolution varies from 9% at a dijet mass of 0.7 TeV to 4.5% at 5 TeV.

57 CMS will record events that pass a first level trigger and a high level trigger. For  
58 an instantaneous luminosity of  $10^{32} \text{ cm}^{-2}\text{s}^{-1}$ , consider three event samples collected by  
59 requiring at least one jet in the high level trigger with corrected transverse energy above  
60 60, 120 and 250 GeV, prescaled by factors of 2000, 40 and 1, respectively. For an integrated  
61 luminosity of  $100 \text{ pb}^{-1}$ , the three event samples will effectively correspond to 0.05, 2.5,  
62 and  $100 \text{ pb}^{-1}$ . The first event sample will be used to measure the trigger efficiency of the  
63 second sample. The last two event samples will be used to study dijets of mass above 330  
64 and 670 GeV, respectively, where the trigger efficiencies are expected to be higher than  
65 99% [9].

66 Backgrounds from cosmic-rays, beam halo, and detector noise are expected to occa-  
67 sionally produce events with large or unbalanced energy depositions. They will be removed  
68 by requiring  $\cancel{E}_T / \sum E_T < 0.3$  and  $\sum E_T$  less than 14 TeV, where  $\cancel{E}_T$  ( $\sum E_T$ ) is the mag-  
69 nitude of the vector (scalar) sum of the transverse energies measured by all calorimeter  
70 towers in the event. This cut is estimated to be more than 99% efficient for both QCD

71 jet events and the signals of new physics considered. In the high  $p_T$  region relevant for  
72 this search, jet reconstruction is fully efficient.

73 CMS plans to search for contact interactions using the jet  $p_T$  distribution. Figure 1  
74 shows the inclusive jet differential cross section as a function of  $p_T$ , for jets with  $|\eta| <$   
75 1. Considering first the QCD processes, the reconstructed and corrected quantities are  
76 compared with the QCD prediction for generated jets. After corrections, the reconstructed  
77 and generated distributions agree. The ratio of the corrected jet cross section to the  
78 generated jet cross section varies between 1.2 at  $p_T = 100$  GeV and 1.05 at  $p_T = 500$  GeV,  
79 and remains roughly constant for higher  $p_T$ . The deviation of this ratio from 1 is attributed  
80 to the smearing effect of the jet  $p_T$  resolution on the steeply falling spectrum. The  
81 measured spectrum could be further corrected for resolution smearing, and this ratio from  
82 Monte Carlo is an estimate of the size of that correction. The measurement uncertainties  
83 are predominantly systematic. The inset in figure 1 shows the effect on the jet rate  
84 of a 10% uncertainty in jet energy correction that could be expected in early running  
85 when only  $10 \text{ pb}^{-1}$  of integrated luminosity have been accumulated. This experimental  
86 uncertainty is roughly ten times larger than the uncertainties from parton distributions,  
87 as estimated using CTEQ6.1 fits [10]. Figure 1 shows that the effect of new physics from a  
88 contact interaction with scale  $\Lambda^+ = 3$  TeV is convincingly above what could be expected  
89 for measurement uncertainties with only  $10 \text{ pb}^{-1}$ . For comparison, a Tevatron search has  
90 excluded contact interactions with scales  $\Lambda^+$  below 2.7 TeV [11].

91 CMS plans to search for narrow dijet resonances using the dijet mass distribution.

92 Figure 2 shows the differential cross section versus dijet mass, where both leading jets  
 93 have  $|\eta| < 1$ , and the mass bins have a width roughly equal to the dijet mass resolution.  
 94 Considering first the QCD processes, the cross section for corrected jets agrees with the  
 95 QCD prediction from generated jets. To determine the background shape either the  
 96 Monte Carlo prediction or a parameterized fit to the data can be used. The inset to  
 97 figure 2 shows a simulation of narrow dijet resonances with a  $q^*$  production cross section.  
 98 This is compared to the QCD statistical uncertainties including trigger prescaling. This  
 99 shows that with an integrated luminosity of  $100 \text{ pb}^{-1}$  a  $q^*$  dijet resonance with a mass  
 100 of 2 TeV would produce a convincing signal above the statistical uncertainties from the  
 101 QCD background. For comparison, a Tevatron search has excluded  $q^*$  dijet resonances  
 102 with mass,  $M$ , below 0.87 TeV [12]. The heaviest dijet resonances that CMS can discover  
 103 (at five standard deviations) with  $100 \text{ pb}^{-1}$  of integrated luminosity, using this search  
 104 technique and including the expected systematic uncertainties [13, 14], are: 2.5 TeV for  
 105  $q^*$ , 2.2 TeV for axiguons [15] or colorons [16], 2.0 TeV for  $E_6$  diquarks [17], and 1.5 TeV  
 106 for color octet technirhos [18]. Studies of the jet  $\eta$  cut have concluded that the optimal  
 107 sensitivity to new physics is achieved with  $|\eta| < 1.3$  for a 2 TeV spin 1 dijet resonance  
 108 decaying to  $q\bar{q}$  [8].

109 CMS plans to search for both contact interactions and dijet resonances using the dijet  
 110 ratio,  $r = N(|\eta| < 0.7)/N(0.7 < |\eta| < 1.3)$ , where  $N$  is the number of events with both jets  
 111 in the specified  $|\eta|$  region. The dijet ratio is sensitive to the dijet angular distribution. For  
 112 the QCD processes, the dijet ratio is the same for corrected jets and generated jets, and

113 is constant at  $r = 0.5$  for dijet masses up to 6 TeV [8]. Figure 3 shows the dijet ratio from  
 114 contact interactions and dijet resonances, compared to the expected statistical uncertainty  
 115 on the QCD processes, for  $100 \text{ pb}^{-1}$  of integrated luminosity, including trigger prescaling.  
 116 The signal from a contact interaction with scale  $\Lambda^+ = 5 \text{ TeV}$  rises well above the QCD  
 117 statistical errors at high dijet mass. Systematic uncertainties in the dijet ratio are expected  
 118 to be small, since they predominantly cancel in the ratio as previously reported [13, 19].  
 119 Using the dijet ratio, CMS can discover a contact interaction at scale  $\Lambda^+ = 4, 7$  and  $10$   
 120 TeV with integrated luminosities of 10, 100, and  $1000 \text{ pb}^{-1}$ , respectively [8]. The signal  
 121 from a 2 TeV spin  $1/2$   $q^*$  produces a convincing peak in the dijet ratio, because it has  
 122 a significant rate and a relatively isotropic angular distribution compared to the QCD  
 123  $t$ -channel processes. Fixing the cross section of the 2 TeV dijet resonance for  $|\eta| < 1.3$   
 124 at  $13.6 \text{ pb}$  (from the  $q^*$  model), the dijet ratio in the presence of QCD background  
 125 increases by approximately 6% when considering a spin 2 resonance decaying to both  
 126  $q\bar{q}$  and  $gg$  (such as a Randall-Sundrum graviton [20]), and the dijet ratio decreases by  
 127 approximately 4% when considering a spin 1 resonance decaying to  $q\bar{q}$  (such as a  $Z'$ ,  
 128 axigluon, or coloron) [8]. Hence, the sensitivity to a 2 TeV dijet resonance depends  
 129 only weakly on the spin of the resonance. Nevertheless, with sufficient luminosity, this  
 130 simple measure of the dijet angular distribution, or a more complete evaluation of the  
 131 angular distribution, can be used to see these small variations and infer the spin of a dijet  
 132 resonance.

133 In conclusion, CMS plans to use measurements of rate as a function of jet  $p_T$  and dijet

134 mass, as well as a ratio of dijet rates in different  $\eta$  regions, to search for new physics in the  
135 data sample collected during early LHC running. With integrated luminosity samples in  
136 the range 10–100 pb<sup>-1</sup>, CMS will be sensitive to contact interactions and dijet resonances  
137 beyond those currently excluded by the Tevatron.

138 We thank the staffs at CERN and other CMS Institutes, and acknowledge support  
139 from: Austrian Federal Ministry of Science and Research; FNRS and FWO (Belgium);  
140 CNPq and FAPERJ (Brazil); Bulgarian Ministry of Education and Science; CERN; CAS  
141 and NSFC (China); Croatian Ministry of Science and Technology; University of Cyprus;  
142 Estonian Academy of Sciences and NICPB; Academy of Finland, Finish Ministry of Ed-  
143 ucation and Helsinki Institute of Physics; CEA and CNRS/IN2P3 (France); BMBF and  
144 DESY (Germany); General Secretariat for Research and Technology (Greece); NKTH  
145 (Hungary); DAE and DST (India); IPM (Iran); UCD (Ireland); INFN (Italy); KICOS  
146 (Korea); CINVESTAV, CONACYT, and UASLP-FAI (Mexico); PAEC (Pakistan); State  
147 Commission for Scientific Research (Poland); FCT (Portugal); JINR (Armenia, Belarus,  
148 Georgia, Ukraine, Uzbekistan), Ministry of Science and Technologies of the Russian Fed-  
149 eration, Russian Ministry of Atomic Energy; Ministry of Science and Environmental Pro-  
150 tection of the Republic of Serbia; Oficina de Ciencia y Tecnologia (Spain); ETHZ, PSI,  
151 University of Zurich (Switzerland); National Science Council (Taipei); TAEA (Turkey);  
152 STFC (United Kingdom); DOE and NSF (USA).

## References

- 153
- 154 [1] E. Eichten, K. Lane and M. E. Peskin, Phys. Rev. Lett. **50**, 811 (1983).
- 155 [2] U. Baur, I. Hinchliffe and D. Zeppenfeld, Int. J. Mod. Phys. **A2**, 1285 (1987).
- 156 [3] T. Sjostrand, L. Lonnblad, S. Mrenna, hep-ph/0108264.
- 157 [4] CMS Collaboration, “The CMS experiment at the CERN LHC” (accepted for publi-  
158 cation in JINST).
- 159 [5] CMS Collaboration, Physics TDR Volume I, CERN-LHCC-2006-001.
- 160 [6] S. Agostinelli *et al.* (GEANT4 Collaboration), Nucl. Instrum. Meth. **A506**, 250-303  
161 (2003).
- 162 [7] CMS Collaboration, CMS Physics Analysis Summary JME-07-003 (2008). at  
163 <http://cms-physics.web.cern.ch/cms-physics/public/JME-07-003-pas.pdf> .
- 164 [8] CMS Collaboration, CMS Physics Analysis Summary SBM-07-001 (2007) at  
165 <http://cms-physics.web.cern.ch/cms-physics/public/SBM-07-001-pas-v3.pdf> .
- 166 [9] S. Esen and R. Harris, CMS Note 2006/069.
- 167 [10] J. Pumplin *et al.* (CTEQ Collaboration), JHEP **07**, 012 (2002).
- 168 [11] B. Abbott *et al.* (D0 Collaboration), Phys. Rev. Lett. **82**, 2457 (1999).
- 169 [12] K. Hatakeyama *et al.* (CDF Collaboration) recent public results at  
170 [http://www-cdf.fnal.gov/physics/exotic/r2a/20080214.mjj\\_resonance\\_1b/](http://www-cdf.fnal.gov/physics/exotic/r2a/20080214.mjj_resonance_1b/).

- 171 [13] CMS Collaboration, *J. Phys. G: Nucl. Part. Phys.* **34**, 995 (2006).
- 172 [14] K. Gumus, N. Akchurin, S. Esen and R. Harris, CMS Note 2006/070.
- 173 [15] J. Bagger, C. Schmidt and S. King, *Phys. Rev. D* **37**, 1188 (1988).
- 174 [16] E. Simmons, *Phys. Rev. D* **55**, 1678 (1997).
- 175 [17] J. Hewett and T. Rizzo, *Phys. Rep.* **183**, 193 (1989) and references therein.
- 176 [18] K. Lane and S. Mrenna, *Phys. Rev. D* **67**, 115011 (2003).
- 177 [19] S. Esen and R. Harris, CMS Note 2006/071.
- 178 [20] L. Randall and R. Sundrum, *Phys. Rev. Lett.* **83**, 3370 (1999).

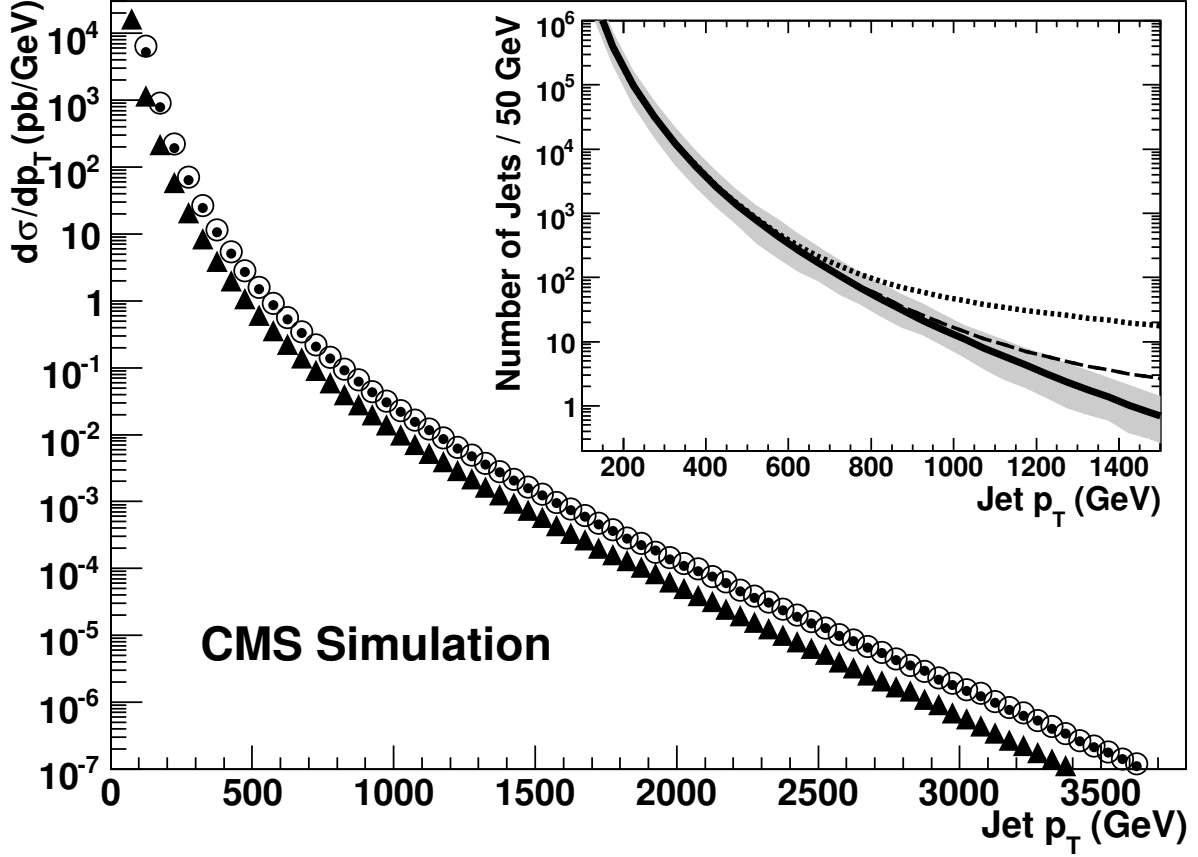


Figure 1: The inclusive jet  $p_T$  differential cross section expected from QCD for  $|\eta| < 1$ , for generated jets (points), reconstructed jets (triangles), and corrected jets (open circles). The inset shows the number of generated jets expected in 50 GeV bins for an integrated luminosity of  $10 \text{ pb}^{-1}$ . The standard QCD processes (solid) are compared to a signal from contact interactions with scale  $\Lambda^+ = 3 \text{ TeV}$  (dotted) and  $5 \text{ TeV}$  (dashed). The shaded band represents the effect of a 10% uncertainty on the jet energy scale.

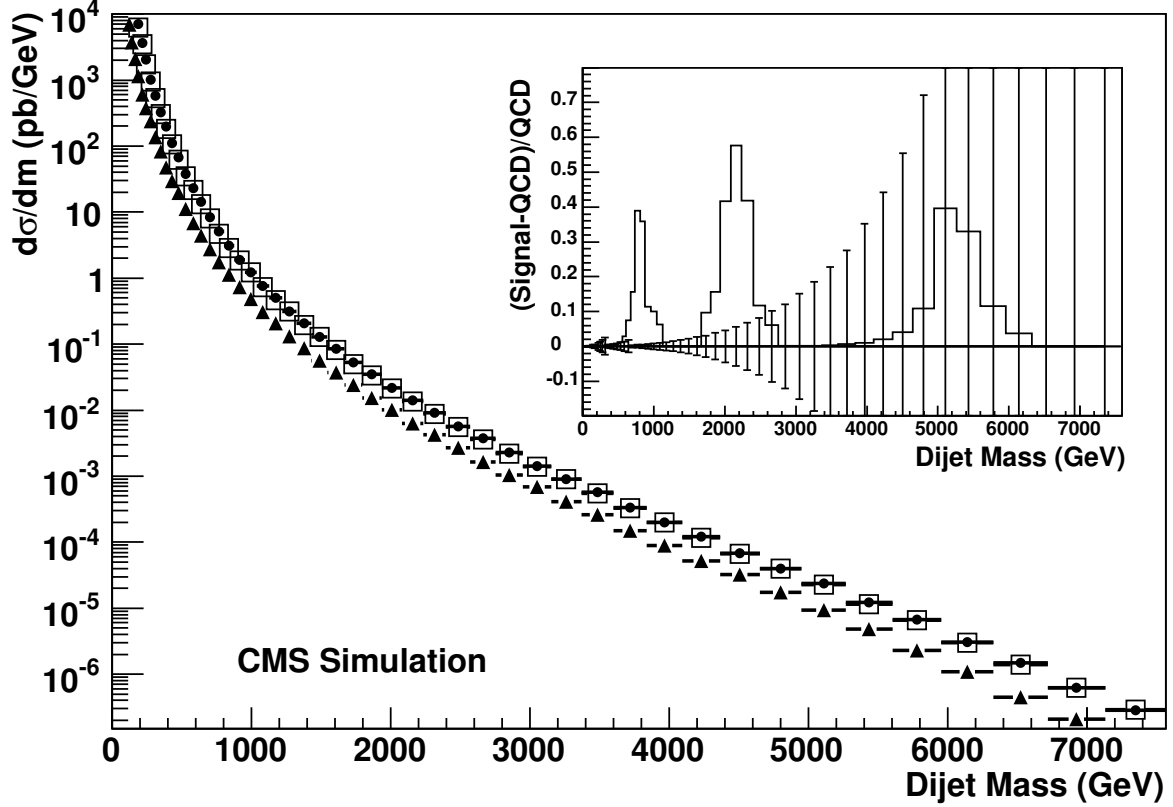


Figure 2: The dijet mass differential cross section expected from QCD for  $|\eta| < 1$  vs. dijet mass,  $m$ , for generated jets (points), reconstructed jets (triangles), and corrected jets (open boxes). The inset shows dijet resonances reconstructed using corrected jets coming from  $q^*$  signals [14] of mass 0.7, 2, and 5 TeV. The fractional difference (histogram) between the  $q^*$  signal and the QCD background is compared to the QCD statistical error (vertical bars) for an integrated luminosity of  $100 \text{ pb}^{-1}$ .

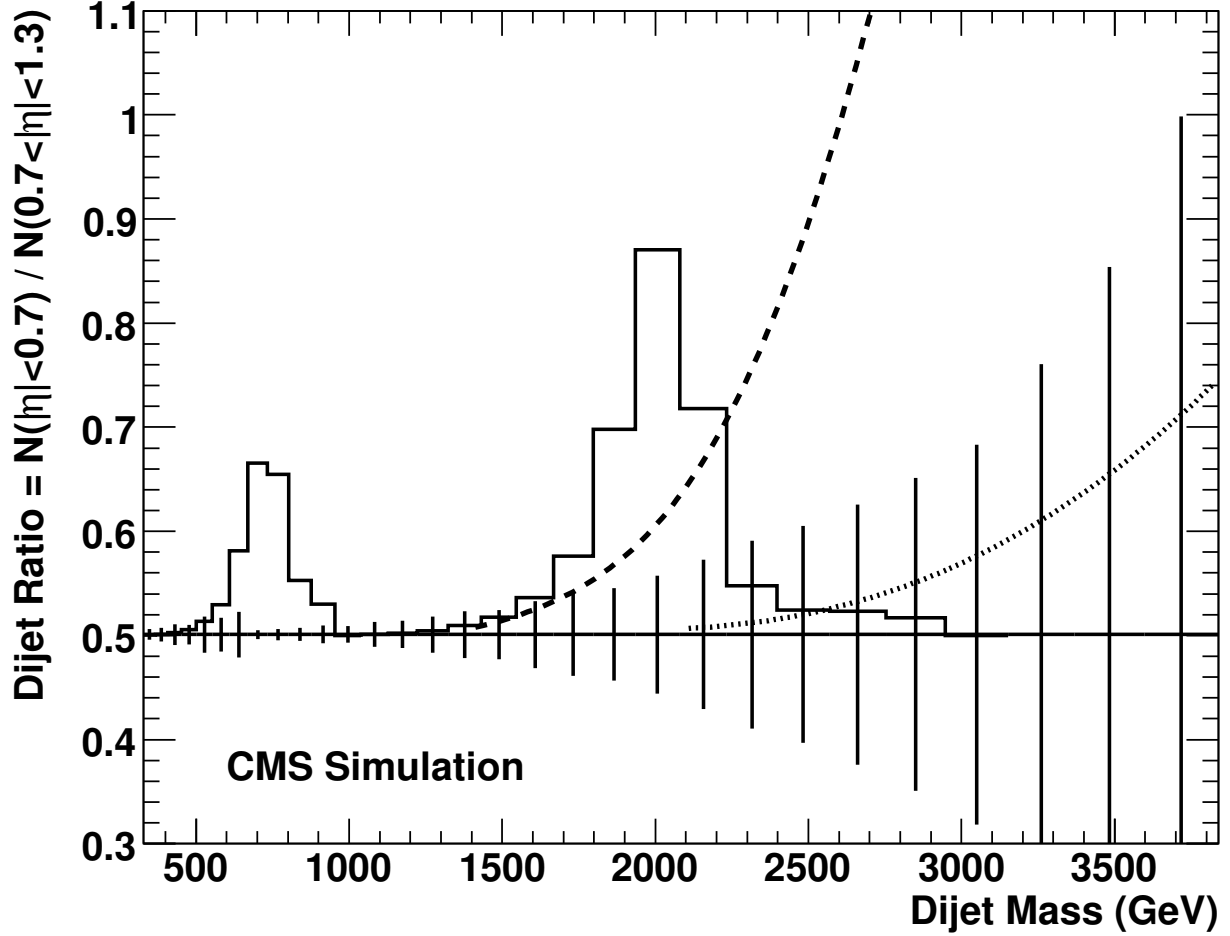


Figure 3: The dijet ratio for corrected jets expected from QCD (horizontal line), with statistical uncertainties (vertical bars) for an integrated luminosity of  $100 \text{ pb}^{-1}$ , is compared to QCD + contact interaction signals with a scale  $\Lambda^+ = 5 \text{ TeV}$  (dashed) and  $10 \text{ TeV}$  (dotted), as well as to QCD + dijet resonance signals (histogram) with  $q^*$  masses of  $0.7$  and  $2 \text{ TeV}$ .